SANDIA REPORT
SAND2009-4932
Unlimited Release
Printed August, 2009

On the Dissolution of Iridium by Aluminum

John C. Hewson

Prepared by
Sandia National Laboratories
Albuquerque, New Mexico 87185 and Livermore, California 94550

Sandia is a multiprogram laboratory operated by Sandia Corporation,
a Lockheed Martin Company, for the United States Department of Energy's
National Nuclear Security Administration under Contract DE-AC04-94AL85000.

Approved for public release; further dissemination unlimited.

Sandia National Laboratories

Issued by Sandia National Laboratories, operated for the United States Department of Energy by Sandia Corporation.

NOTICE: This report was prepared as an account of work sponsored by an agency of the United States Government. Neither the United States Government, nor any agency thereof, nor any of their employees, nor any of their contractors, subcontractors, or their employees, make any warranty, express or implied, or assume any legal liability or responsibility for the accuracy, completeness, or usefulness of any information, apparatus, product, or process disclosed, or represent that its use would not infringe privately owned rights. Reference herein to any specific commercial product, process, or service by trade name, trademark, manufacturer, or otherwise, does not necessarily constitute or imply its endorsement, recommendation, or favoring by the United States Government, any agency thereof, or any of their contractors or subcontractors. The views and opinions expressed herein do not necessarily state or reflect those of the United States Government, any agency thereof, or any of their contractors.

Printed in the United States of America. This report has been reproduced directly from the best available copy.

Available to DOE and DOE contractors from
U.S. Department of Energy
Office of Scientific and Technical Information
P.O. Box 62
Oak Ridge, TN 37831

Telephone: (865) 576-8401
Facsimile: (865) 576-5728
E-Mail: reports@adonis.osti.gov
Online ordering: http://www.osti.gov/bridge

Available to the public from
U.S. Department of Commerce
National Technical Information Service
5285 Port Royal Rd.
Springfield, VA 22161

Telephone: (800) 553-6847
Facsimile: (703) 605-6900
E-Mail: orders@ntis.fedworld.gov
Online order: http://www.ntis.gov/help/ordermethods.asp?loc=7-4-0#online

SAND2009-4932
Unlimited Release
Printed August, 2009

On the Dissolution of Iridium by Liquid Aluminum

John C. Hewson[1]
Fire and Aerosol Sciences Department
Sandia National Laboratories
Albuquerque, NM 87185-0836

Abstract

The potential for liquid aluminum to dissolve an iridium solid is examined. Substantial uncertainties exist in material properties, and the available data for the iridium solubility and iridium diffusivity are discussed. The dissolution rate is expressed in terms of the regression velocity of the solid iridium when exposed to the solvent (aluminum). The temperature has the strongest influence in the dissolution rate. This dependence comes primarily from the solubility of iridium in aluminum and secondarily from the temperature dependence of the diffusion coefficient. This dissolution mass flux is geometry dependent and results are provided for simplified geometries at constant temperatures. For situations where there is negligible convective flow, simple time-dependent diffusion solutions are provided. Correlations for mass transfer are also given for natural convection and forced convection. These estimates suggest that dissolution of iridium can be significant for temperatures well below the melting temperature of iridium, but the uncertainties in actual rates are large because of uncertainties in the physical parameters and in the details of the relevant geometries.

[1] Email address: jchewso@sandia.gov

Introduction

For deep space probes and other extraterrestrial vehicles it is sometimes necessary to employ radio-isotopic thermoelectric generators (RTG) as power sources. The RTG carries a small quantity of plutonium for which the radioactive decay provides heat to drive thermoelectric power generation needed for on-board equipment. It is necessary to consider any hazards associated with the presence of radioactive materials, and for every launch of a space vehicle carrying an RTG a safety analysis is conducted. One contribution to the net hazard associated with a launch is the possibility that the plutonium present in the RTG will be exposed to a serious fire environment associated with the burning of the launch vehicle propellants. To protect the plutonium from hazards, plutonium pellets are encased within iridium cladding that is encased within a graphite impact shell (GIS). The present document addresses one aspect of what might happen if the GIS is compromised in some way and if the iridium cladding is exposed to the propellant fire environment.

The melting temperature of iridium at 2720 K (2447 C) is relatively high, but this is still within the range of temperatures that are obtainable in propellant fires. Of particular concern is the solid-propellant fire environment in which these high temperatures can be sustained for minutes as large propellant fragments burn, possibly in the vicinity of the clad plutonium pellets. Also present in a solid-propellant fire environment are aluminum particles from the propellant. These particles are included within the solid propellant to increase specific thrust. In a fire scenario when the propellant burns at ambient pressure (as opposed to very high pressures within the rocket motor) aluminum particles agglomerate before leaving the propellant surface, and in the agglomerated state they are particularly prone to deposit on surrounding surfaces as largely unoxidized aluminum. This report focuses on how the presence of aluminum particles depositing on an iridium surface affects the structural integrity of the iridium, in particular its propensity to dissolve at high temperatures. As is discussed in the following, this dissolution has the effect of reducing the protective nature of the iridium at temperatures well below the iridium melting temperature. The present report addresses the question of just how much iridium dissolution is likely to occur and at what temperatures.

Material Properties

When two materials with differing melting temperatures are brought together, one in the liquid state and the other in the solid state, it is possible for the liquid phase to dissolve the solid phase. This is exemplified in the dissolution of salt in water. In the present work, we consider the dissolution of iridium (Ir) in liquid aluminum (Al). A phase diagram for this system is shown in **Figure 1** [1, 2]. The melting point of aluminum is 933 K (660 °C) while that of iridium is 2720 K (2447 °C). The uppermost line in **Figure 1** extending between the two melting temperatures of the pure components is referred to as the liquidus line. For a given composition, states above the liquidus line are pure liquid. Viewed in the other direction, the composition corresponding to the liquidus line at a given temperature shows the solubility of iridium in the liquid solution. For example, for temperatures on the order of 1800 C, the solubility of Ir in atomic percent is on the order of 38%.

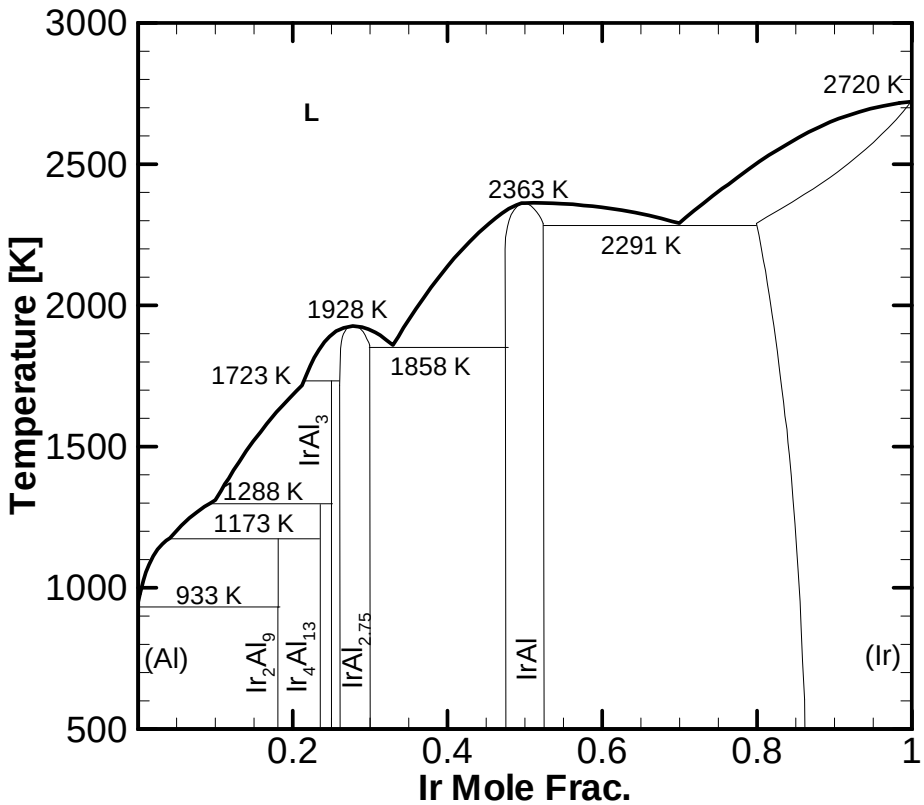

Figure 1. Aluminum-iridium phase diagram with liquidus line emphasized [1, 2].

The solubility obtained from the liquidus line in **Figure 1** [1, 2] is plotted as a function of temperature in **Figure 2** where it is labeled (Okamoto, 2000). A rough approximation can be obtained by fitting an Arrhenius form expression to the curve for mole fractions exceeding 0.05 and this results in $X_0 \approx 8.123\exp(-6118/T)$. This curve fit will not be used in the subsequent results presented, but it is noteworthy that the activation energy for the solubility in this expression is approximately 51 kJ/mol. More recently, the liquidus line has been measured at low Ir mole fractions [3], and these results are also shown in **Figure 2** labeled (Ode, 2008). This has been curve fit to an Arrhenius form, $X_0 \approx 124.7\exp(-11548/T)$, suitable for mole fractions up to 0.3; this gives an effective activation energy of approximately 96 kJ/mol. Comparing available phase diagrams over the past two decades shows considerable change in the iridium-aluminum phase diagram suggesting some uncertainty in this quantity. For example, the phase diagram that was available prior to 2000 was substantially less detailed [4]. A portion of the solubility curve from this older phase diagram is also shown in **Figure 2** labeled as (Predel, 1991). While the recent phase diagrams [1-3] are used exclusively in the present work, the substantial change in this recent development is indicative of potential uncertainties in this system. In addition, since the liquidus line from Ref. [3] is based on measurements for Ir mole fractions below 0.3, we recommend employing that as a nominal value for the solubility and

using the higher solubility suggested by Refs. [1, 2] as a measure of uncertainty. References [1, 2] are recommended for higher mole fractions ($X_0 > 0.3$).

The diffusivity of Ir in Al has not been found in the literature, so a review of other available values is employed. Typically, the diffusion coefficient is expressed in the form $D = D_0 \exp(-Q/RT)$. A review of available data for trace species diffusion in liquid aluminum and extrapolation of that data to other species is available in [5]. Based on the available data, diffusion coefficients in liquid aluminum have activation energies, *Q*, in the range of 20-40 kJ/mol; this is a substantial temperature dependence, but not as large as the temperature dependence associated with the iridium solubility as indicated by the curve fits in the previous paragraph. Since the diffusion coefficient of iridium is not given, we use the diffusion coefficient of cobalt (D_0 = 8.13e-8 m^2/s and Q = 27.4 kJ/mole) because this has the same relative valence [5]. Since the iridium atom is larger, the iridium diffusivity is likely smaller than that of cobalt. For comparison, we plot the diffusion coefficients of cobalt and iron in

Figure 3. We suggest that there is at least a factor of two uncertainty in "iridium" diffusion coefficient used here (that for cobalt).

When there is flow of the liquid, the viscosity becomes an important parameter. In liquids, the viscosity tends to decrease as the temperature goes up, a behavior that is opposite that of the diffusivity. For liquid aluminum, the viscosity is taken to be μ=1.492e-4 exp(1984.5 / T) [6].

The ratio of the species diffusivity to the viscosity is known as the Schmidt number, $Sc = \mu/\rho D$. For metals the Schmidt number tends to be large, but since the viscosity decreases with temperature while the diffusivity increases with temperature, the Schmidt number is sharply decreasing with temperature. At the aluminum melting temperature of 933 K and using the diffusivity of cobalt and the viscosity of aluminum, the Schmidt number is nearly 250, but above 2000 K it is less than twelve as indicated in

Figure 3.

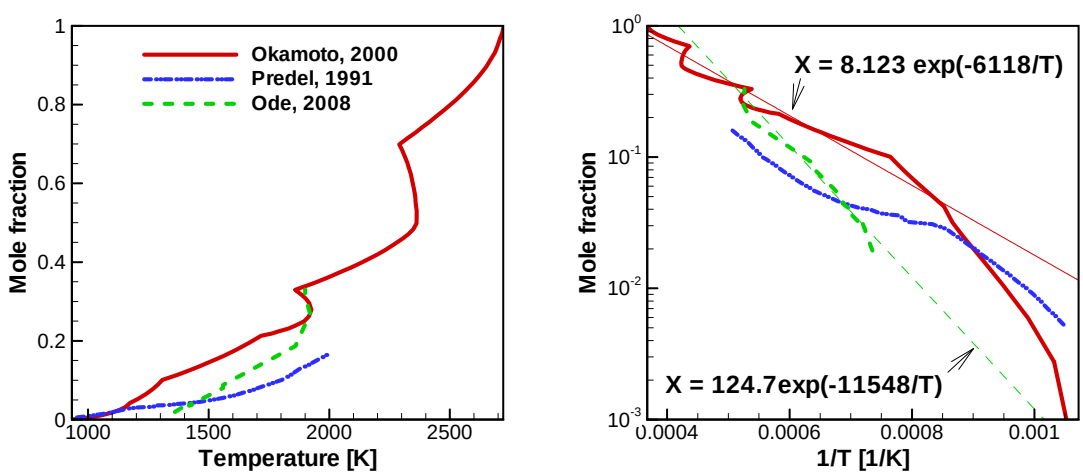

Figure 2. The solubility of Ir in liquid Al expressed in terms of mole fraction of atomic Ir as a function of temperature. The solid line is obtained from the Okamoto (2000) phase diagram and the dashed line is from the Ode et al. (2008) phase diagram. Arrhenius form curve fits to these data are shown as fine lines. For the purpose of comparison, the solubility from the phase diagram of Predel (1991) is also shown.

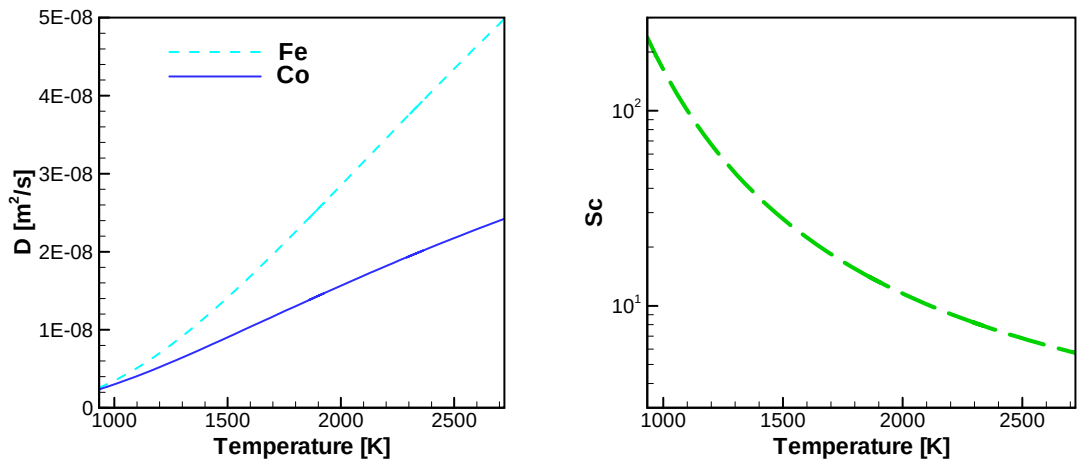

Figure 3. Diffusion coefficients of cobalt and iron in liquid aluminum are indicated on the left panel. The right panel shows the Schmidt number for cobalt in aluminum.

Dissolution rate model

We are interested in the rate of dissolution of solid iridium in liquid aluminum and consider an interface with solid iridium (solute) on one side ($y < 0$) and liquid aluminum (solvent) on the other ($y > 0$). The mole fraction of the iridium in the liquid phase at the interface is the solubility, given by the liquidus line, for the given interface temperature.
The mass flux at the interface is described by the boundary condition [7]

$$\rho_{\mathrm{Ir}} v_{\mathrm{Ir}} = \rho_0 v_0 = -\frac{\rho_0 D}{1 - X_0} \frac{dX}{dy}\bigg|_0 \qquad (1)$$

where the regression velocity of the surface is v_{Ir}, the liquid-phase Stefan velocity is v_0, the density is ρ, the mole fraction of Ir in the liquid phase is X, the subscript 0 denotes conditions on the liquid side of the surface and D is the diffusion coefficient of Ir in liquid Al at the interface temperature. Note that a coordinate system fixed to the interface is selected. The regression velocity of the surface, v_{Ir}, is the quantity of interest here and the density ratio $\rho_0 / \rho_{\mathrm{Ir}}$ is computed from

$$\frac{\rho_0}{\rho_{\mathrm{Ir}}} = \frac{\rho_{\mathrm{Al}}}{(1 - X_0)\rho_{\mathrm{Ir}} + X_0 \rho_{\mathrm{Al}}}. \qquad (2)$$

The pure component densities are estimated to be $\rho_{\mathrm{Al}} = 2226$ kg/m^3 and $\rho_{\mathrm{Ir}} = 21810$ kg/m^{3}for the present paper, but this neglects thermal expansion. Both X_0 and D are strong functions of temperature (see Material Properties section).

Because the Prandtl numbers of liquid metals are small ($O(10^{-2})$) and the Schmidt numbers are large ($O(10^2)$), the temperature is much more uniform than the concentration field and can be assumed to be uniform to first-order in space, but varying in time. For simplicity, all example solutions given in the present will use a fixed temperature; that is, only solutions for the quasi-

steady problem with negligible temperature variations will be given here. Further, the aluminum layer into which the iridium dissolves will be assumed to be sufficiently thick that it does not begin to saturate with dissolved iridium. In the application of these models, the two temporal variations, that of the deposit temperature and the deposit thickness, may be significant, but in the case of continually rising temperatures and continually increasing aluminum layer thickness, the present assumptions may provide sufficiently quantitative estimates of the dissolution rate.

The gradient at the surface that appears in Eq. (1) depends on the geometry and the prevailing flow field in the dissolution process, but will be expressed here in terms of an effective mass transfer coefficient defined in terms of a Sherwood number, *Sh*, and a characteristic length scale, *L*,

$$\frac{Sh}{L}\left(X_0 - X_\infty\right) = -\left.\frac{dX}{dy}\right|_0 \tag{3}$$

where X_∞ is the far-field or average mole fraction of iridium in the liquid (assumed to be zero for all results in this paper). Given this definition, the dissolution rate is expressed as

$$v_{\mathrm{Ir}} = \frac{\rho_0}{\rho_{\mathrm{Ir}}} v_0 = \frac{Sh\ D}{L}\left(\frac{\rho_{\mathrm{Al}}}{(1-X_0)\rho_{\mathrm{Ir}} + X_0\rho_{\mathrm{Al}}}\right)\frac{X_0 - X_\infty}{1-X_0}\,. \tag{4}$$

Results for simplified configurations

A variety of configurations could lead to a wide range of Sherwood numbers. Even if there is no flow of the aluminum so that there are no convective enhancements, with temperature variation in time, the dissolution profile does not admit an analytical solution. However, a variety of empirical and analytically derived expressions for the Sherwood numbers are available in the literature.

Dissolution with no convective flow

Since it is useful to obtain estimates, further simplifications are employed here including the assumptions that the temperature is constant and that the depth of the aluminum solvent is effectively infinite. Here infinite depth is defined in the context of the diffusion thickness, $(Dt)^{1/2}$, plotted in **Figure 4** for times of one minute and ten minutes; clearly deposits that are several centimeters and greater can be considered to have effectively infinite depth over ten minute durations. With these simplifications, the configuration is analogous to the well-known heat-conduction in a semi-infinite plate problem [8]. The solution in terms of Eq. (3) is then

$$\left.\frac{dX}{dy}\right|_0 = -\frac{\left(X_0 - X_\infty\right)}{\left(\pi Dt\right)^{1/2}} \quad \text{or} \quad \frac{Sh}{L} = \frac{1}{\left(\pi Dt\right)^{1/2}}\,. \tag{5}$$

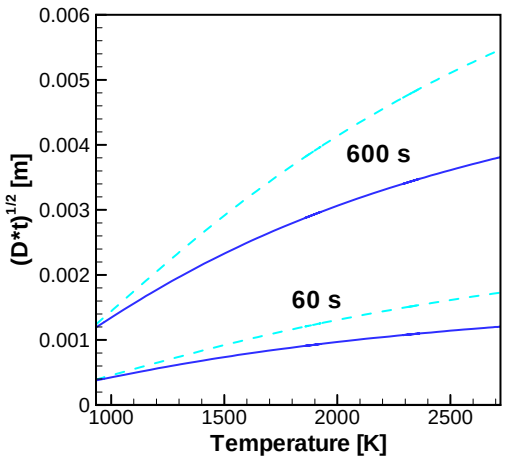

Figure 4. Diffusion coefficients of cobalt and iron in liquid aluminum.

Using this in Eq. (4) shows that the dissolution rate at constant temperature into a semi-infinite solvent is

$$v_{\mathrm{Ir}} = \frac{\rho_0}{\rho_{\mathrm{Ir}}} v_0 = \sqrt{\frac{D}{\pi t}} \left(\frac{\rho_{\mathrm{Al}}}{(1-X_0)\rho_{\mathrm{Ir}} + X_0 \rho_{\mathrm{Al}}} \right) \frac{X_0 - X_\infty}{1 - X_0} . \tag{6}$$

This regression rate is plotted in Figure 5 **at times of 1 s and 60 s using the various solubilities of Ir in Al from the liquidus lines (phase diagrams) indicated in** Figure 2**. The recommended solubilities are those of Ode (2008) where those measurements are available and Okamoto (2000) otherwise. These results use the diffusivity of cobalt (**

Figure 3). Integrating over time, the thickness dissolved is

$$\Delta_{\mathrm{Ir}} = 2\sqrt{\frac{Dt}{\pi}} \left(\frac{\rho_{\mathrm{Al}}}{(1-X_0)\rho_{\mathrm{Ir}} + X_0 \rho_{\mathrm{Al}}} \right) \frac{X_0 - X_\infty}{1 - X_0} \tag{7}$$

These values are also plotted in **Figure 5** (right panel) at times of 1 s, 60 s and 3600 s using the various solubilities of Ir in Al. The range in solubilities, along with uncertainties in the diffusion coefficients, suggests a dissolution uncertainty approaching an order of magnitude. However, the strong temperature dependence of the regression rate suggests that only certain temperature ranges are significant. For example, millimeter-scale dissolution only becomes significant for temperatures exceeding 1930 K (above the melting temperature of $IrAl_{2.75}$). Of particular importance is the jump in regression rates associated with passing the melting temperature of IrAl (2363 K in **Figure 1**). Experiments with good temperature control can presumably measure dissolution rates and jumps in the dissolution rate around these temperatures to reduce uncertainty and to identify temperatures at which the dissolution rates change substantially.

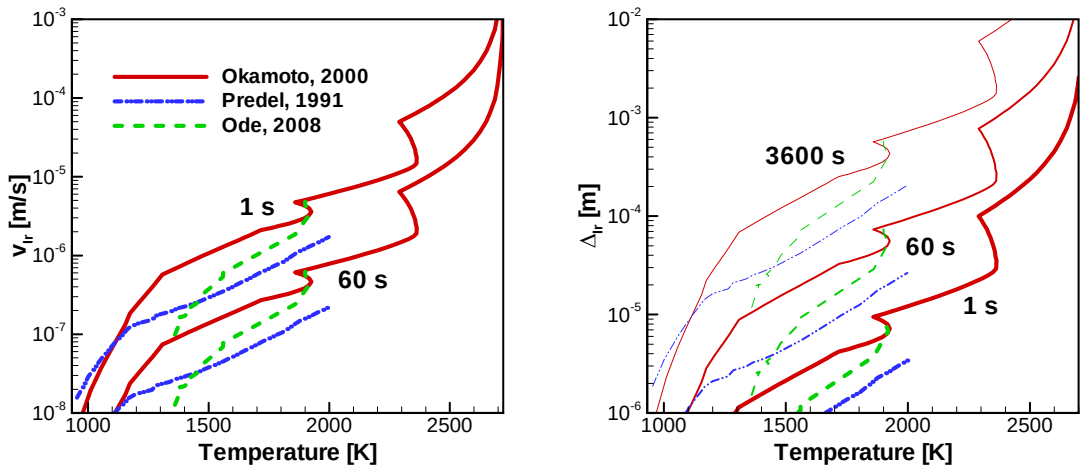

Figure 5. In the left panel, the regression rate of Ir in liquid Al expressed as a function of temperature for stagnant diffusion at times of 1 s and 60 s; the regression rates are reduced in time so that the regression rates at 60 s are below those at 1 s. In the right panel, the integrated iridium thickness dissolved is indicated for 1 s, 60 s and 3600 s; integrated iridium dissolution thickness increases with time so that regression rates at longer times are greater. To indicate the dependence on the solubility, solubilities from various phase diagrams are employed. The solid line is obtained from the Okamoto (2000) phase diagram and the dashed line is from the Ode et al. (2008) phase diagram. For the purpose of comparison, the solubility from the phase diagram of Predel (1991) is also shown.

Solutions are also available for aluminum solvents of finite thickness in the form of series solutions [8] but are not repeated here for brevity. When the temperature is allowed to vary, numerical solutions may be employed. The previous paragraphs focused on situations where there was no flow of the liquid metals. In reality, flow can substantially increase the dissolution rates through either forced or natural convection. Here we draw on other work to address two possible scenarios: one with natural convection and one with forced convection.

Dissolution with natural convective flow

If the iridium surface is vertically oriented, then natural convection is a potential means of enhancing the dissolution process. The dissolved iridium is almost an order of magnitude denser than the solvent aluminum so that the increased density associated with the solute can be substantial. Shiah *et al*. have considered this scenario and have carried out numerical simulations to determine an appropriate Sherwood number [7]. Their results give a semi-empirical correlation for the dissolution rate as a function of the Grashof number

$$Gr_L = \frac{g\left((1-d)X_0\right)L^3}{\nu^2} \tag{8}$$

Here, density changes associated with temperature gradients have been neglected in light of the differences between the Schmidt and Prandtl numbers, g is the acceleration due to gravity, L the characteristic vertical length of the solid substrate, $d = \rho_{\mathrm{Al}} / \rho_{\mathrm{Ir}}$ is the density ratio between the molten substance and the solid substrate and ν is the liquid kinematic viscosity. When the solvent aluminum contains negligible quantities of the solute iridium, the numerical results suggest that the correlation [7]

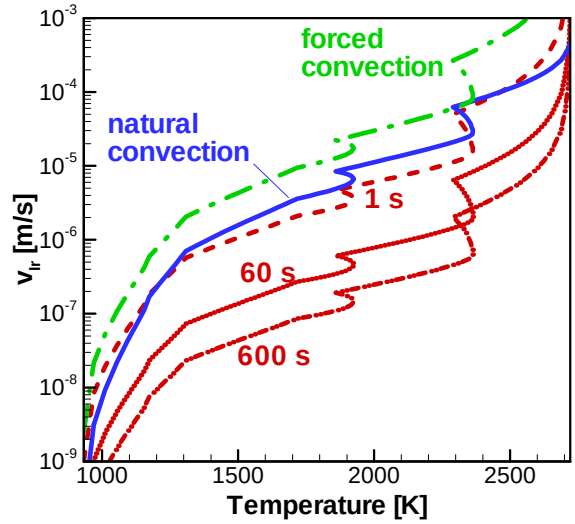

Figure 6. The predicted regression rate of Ir in liquid Al expressed as a function of temperature for natural convection (solid line) and for stagnant diffusion at times of 1 s, 60 s and 600 s (broken lines as labeled). The vertical length scale for natural convection is 1 cm. All Ir solubilities are obtained from Okamoto (2000).

$$v_0 = 0.64\frac{D}{L}\left[1+0.27X_0+0.12X_0^2\right]X_0 Sc^{1/4}Gr_L^{1/4} \qquad (9)$$

is appropriate. (This particular correlation is only valid in the limit where $X_\infty = 0$; see Ref. [7] for the correlation when $X_\infty > 0$.) The combined effect of the vertical length scale appearing in the Grashof number and the *D/L* ratio is a minor $L^{-1/4}$ scaling. Taking the Schmidt number, *Sc*, from the temperature-dependent transport coefficients as in

Figure 3 and the length scale, *L*, to be 10^{-2} m, this is plotted in terms of v_{Ir} in **Figure 6** using the density ratio in Eq. (2). Natural convection essentially puts a lower bound on the dissolution rate for vertically oriented surfaces, and once natural convection becomes dominant, the rate of dissolution will tend to be linear in time. For this parameter set natural convection will be a significant driver for vertical surfaces. Equation (9) gives an integrated regression rate over the vertical surface. The leading edge of the boundary layer, the upper edge in this case, will experience higher rates of dissolution and in future work this should be accounted for.

Dissolution with forced convective flow

In the solid propellant fire environment, strong shear forces may be exerted on the liquid aluminum leading to a forced convective flow of the aluminum over the substrate. In this case, a boundary layer will be formed over the substrate. Enhanced mass transfer in a boundary layer can be correlated using the Schmidt number and Reynolds number, $Re_L = u_\infty L/\nu$, where u_∞ is the mean velocity of the aluminum flowing over the substrate. To determine the mean velocity of aluminum flowing over the substrate, we employ an expression for the overall shear stress on a flat plate in a boundary layer [8]

$$\tau = 1.328\sqrt{\frac{\rho\mu}{L}}u_\infty^{3/2} \tag{10}$$

where τ is the shear stress on the substrate from the boundary layer. From simulations of the flow under a downward burning propellant, shear stresses on the order of 1 to 10 kg/s^2/m are observed. Using a shear stress of $\tau = 3$ kg/s^2/m in Eq. (10) results in $u_\infty \approx 0.3$ m/s. The velocity calculated in Eq. (10) including the temperature dependence of the viscosity is employed in the Reynolds number indicating that Reynolds numbers are moderately large, being $O(10^4)$. For laminar flow, correlations are available for the mass-transfer limited dissolution in textbooks. In a form analogous to Eq. (9), the velocity of the liquid at the interface is [8]

$$v_0 = 0.677\frac{D}{L}Sc^{1/3}Re_L^{1/2}\left(\frac{X_0 - X_\infty}{1 - X_0}\right). \tag{11}$$

As for natural convection, taking the Schmidt number from the relations given in the Material Properties section and the length scale, L, to be 10^{-2} m, the iridium regression rate for forced convection is plotted in terms of v_{Ir} using the density ratio in Eq. (2) in **Figure 6**. There it is clear that forced convection, with the estimated flow velocity of $u_\infty \approx 0.3$ m/s, provides substantial enhancement of the iridium dissolution rate.

Discussion

A series of simple estimates of the dissolution rate for iridium in molten aluminum have been provided. The significance of dissolution rates can be addressed in the context of time and length scales of significance. If we suppose that time and length (iridium thickness) scales of interest are minutes (100-1000 s) and millimeters, then regression rates greater than 10^{-6} m/s are of concern. These occur for a surprisingly large range of temperatures when convective flows are included as indicated in **Figure 6**. It is noted that the regression rates indicated in **Figure 6** are for the Okamoto solubilities [1, 2] that may overestimate the iridium solubility at low temperatures by as much as an order of magnitude when comparing with Ode *et al*. solubilities [3], but this is still within the present range of uncertainties.

It is also noteworthy that the expressions used in the two sections on dissolution in convective flow are based on boundary layers initiated at sharp boundaries. If flow is over a blunt object, the initial thin boundary layer will not exist and a stagnation-flow boundary layer may be more appropriate for this case. Similarly, the expressions for dissolution in the absence of any convection are appropriate for flat surfaces but will be enhanced at corners. Thus, the estimates provided in the previous sections should be considered as only rough estimates for complicated environments (i.e. in an actual solid-propellant fire). The results are useful for identifying the temperature and length scale regimes in which dissolution does become important, however. They are also useful for designing simplified experiments. It is expected, however, that to predict dissolution rates to within an order of magnitude it will be necessary to carry out higher-fidelity numerical simulations of the aluminum flows in various configurations to better identify the effects of more complicated geometry like, for example, well-rounded iridium surfaces. Such capabilities are in development in the context of Sandia's multi-physics code suite, Sierra.

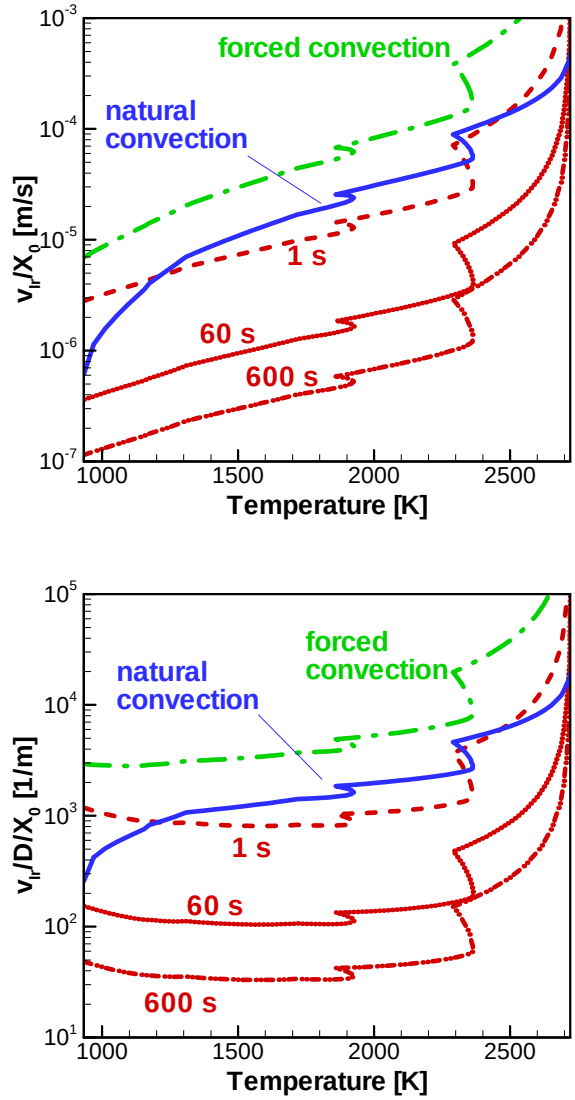

Figure 7. The predicted regression rate of Ir in liquid Al as in Figure 6 but normalized by the leading order dependence on X_0 (top) and by DX_0 (bottom). Line legend as per Figure 6.

Even with the simplifications employed here, it is instructional to understand the dependencies of the iridium regression rates on the various parameters. The leading order dependency for all conditions is the iridium mole fraction, X_0, at the surface of the substrate. This mole fraction varies with temperature over orders of magnitudes as indicated in Figure 2**, and the regression rates all have at least a linear dependence on this quantity. In** Figure 7**, the iridium regression rates have been normalized by X_0 so that the magnitude of the other functional dependencies can be seen. The second most significant temperature dependence arises through the diffusion coefficient (for cobalt) shown in**

Figure 3. This is indicated in the lower panel of **Figure 7** where the regression rates are normalized by DX_0. Significant remaining dependencies come from the density ratio in Eq. (2) and the $1/(1- X_0)$ term in the various equations for v_0 (this is implicit in Eq. (9)). The increased

viscosity at lower temperatures also tends to reduce the natural and forced convective flows at low temperatures. In the present work, we have not parametrically varied the boundary layer length scale, *L*, in Eqs. (9) and (11). In all of the shown results, this length scale is assumed to be 10^{-2} m, but the effect of varying this length scale in the simplified boundary layer flow is well known. For example, for natural convection the overall dependence is $v_0 \propto L^{-1/4}$ as can be seen from Eqs. (8) and (9) while for forced convection is $v_0 \propto L^{-1/2}$ (here u_∞ is assumed independent of *L*) from Eq. (11) and the definition of the Reynolds number. Increasing the length scales can lead to reductions in the expected convective dissolution rates, but these dependencies are less than linear.

Summary and Conclusions

The solubility of iridium in liquid aluminum offers the possibility that solid iridium in liquid aluminum can dissolve at temperatures well below the melting temperature of iridium. In this work we have analyzed the parameters that determine the iridium dissolution rate. Of primary importance is the solubility of iridium in liquid aluminum. This information comes from the liquidus line on the Al-Ir phase diagram, but there is substantial variation in the published phase diagrams and liquidus data. The variability suggests that uncertainties in this important parameter can be as great as an order of magnitude where the solubility is small, but these conditions are likely to be less important because the dissolution rate is relatively small for those conditions. At higher solubilities, the uncertainty is estimated to be bounded by 0.15 mole fraction. Also significant is the diffusivity of iridium in aluminum. Since data is not available for this pair, we have employed the iso-valent cobalt diffusivity and compared it with the diffusivity of iron to give a measure of the uncertainty across materials; this suggests as much as a factor of two uncertainty in the diffusion coefficients.

Dissolution can occur in various flow configurations. Estimates of dissolution rates for simplified geometries are given for configurations with no convective flow (pure diffusion) and for configurations where natural and forced convective flow occurs over a boundary layer with a sharp edge. These provide estimates of the range of dissolution rates that are possible at various temperatures.

Acknowledgements

This work was supported by a grant from the Air Force Safety Center under the direction of Dr. Firooz Allahdadi. Sandia is a multiprogram laboratory operated by Sandia Corporation, a Lockheed Martin Company, for the United States Department of Energy's National Nuclear Security Administration under Contract DE-AC04-94AL85000.

References

1. Okamoto, H. *Al-Ir phase diagram*. ASM Alloy Phase Diagrams Center 2006 [cited Aug. 2008]; Available from: http://www.asminternational.org/AsmEnterprise/APD.
2. Okamoto, H., *Al-Ir (Aluminum-Iridium).* J. Phase Equilib., 2000. **21**: p. 409.
3. Ode, M., et al., *An investigation of the phase diagram of the Al-Ir binary system.* Intermetallics, 2008. **16**: p. 1171-1178.

4. Predel, B., *Subvolume a: Ac-Au ... Au-Zr*, in *Landolt-Borstein -- Group IV: Physical Chemistry, Vol. 5 of Phase Equilibria, Crystallographic and Thermodynamic Data of Binary Alloys*, O. Madelung, Editor. 1991. p. 168-189.
5. Du, Y., et al., *Diffusion coefficients of some solutes in fcc and liquid Al: critical evaluation and correlation.* Mater. Sci. and Engin. A, 2003. **363**(1-2): p. 140-151.
6. Smithells, C.J., E.A. Brandes, and G.B. Brook, *Smithells light metals handbook* 1998: Butterworth-Heinemann.
7. Shiah, S.W., et al., *Natural convection mass transfer along a dissolution boundary layer in an isothermal binary metallic system.* International Journal of Heat and Mass Transfer, 1998. **41**(23): p. 3759-3769.
8. Bird, R.B., W.E. Stewart, and E.N. Lightfoot, *Transport Phenomena*. 2nd ed. 2007, New York: John Wiley & Sons.

Distribution

Internal:

1 MS 0836, T. L. Aselage, 1514
1 MS 0836, R. R. Rao, 1514
1 MS 0836, D. R. Noble, 1514
1 MS 0836, W. W. Erikson, 1516
2 MS 0836, J. C. Hewson, 1532
1 MS 1135, S. R. Tieszen, 1532
1 MS 0826, W. Gill, 1532
1 MS 1135, V. F. Nicolette, 1532
1 MS 1135, A. Ricks, 1532
1 MS 0836, P. K. Notz, 1541
1 MS 0836, S. P. Domino, 1541
1 MS 0736, D. A. Powers, 6770
1 MS 0747, R. J. Lipinksi, 6774
1 MS 0747, T. J. Bartel, 6774
1 MS 0747, C. W. Morrow, 6774
1 MS 0899 Technical Library, 9536
(electronic copy)

External:

3 Dr. Firooz Allahdadi
HQ AFSC/SES
9700 G Avenue SE
Kirkland Air Force Base
Albuquerque, NM 87117

1 Lyle L. Rutger
Office of Radioisotope Power Systems
NE-34
US Department of Energy
19901 Germantown Road
Germantown, MD 20874

1 Ryan Bechtel
Office of Radioisotope Power Systems
NE-34
US Department of Energy
19901 Germantown Road
Germantown, MD 20874

1 Yale Chang
1E-255
Johns Hopkins University
Applied Physics Laboratory
11100 Johns Hopkins Road
Laurel, MD 20723

1 Mr. Bart Bartram
Tetra Tech NUS, Inc.
20251 Century Boulevard, Suite 200
Germantown, MD 20874-7114

1 Meera Mukunda
Orbital Sciences Corporation
20030 Century Blvd., Suite 102
Germantown, MD 20874

Sandia National Laboratories